

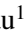



Control-relevant Model Selection for Multiple-Mass Systems

Mathias Tantau¹, Torben Jonsky², Zygimantas Ziaukas¹ and Hans-Georg Jacob¹

¹*Institute of Mechatronic Systems, Leibniz University Hannover, An der Universität 1, 30823 Garbsen, Germany*

²*Lenze SE, Hans-Lenze-Str. 1, 31855 Aerzen, Germany*

{mathias.tantau, zygimatas.ziaukas}@imes.uni-hannover.de, torben.jonsky@lenze.com

Keywords: Control-relevant Model Selection, Model-based Control, Multiple-Mass Systems, Non-parametric Models, Modelless Simulation.

Abstract: Physically motivated parametric models are the basis of several techniques related to control design. Industrial model-based controller tuning methods include pole placement, symmetric optimum and damping optimum. The challenge is that the resulting model-based controller is satisfactory only if the underlying model is appropriate. Typically, a set of potential models is known a priori, but it is not known, which model should be used. So, the critical question in model-based controller tuning is that of model selection. Existing approaches for model selection are mostly based on maximizing accuracy, but there is no reason why the most accurate model should also be the optimal model for control design. Given the overall aim to design a high-performance controller, in this paper the best model is considered as the one that has the potential to give a model-based controller the highest performance. The proposed method identifies parametric candidate models for control design. Then, a nonparametric model is used to predict the actual performance of the various controllers on the real system. A validation with two industry-like testbeds shows success of the method.

1 INTRODUCTION


Physically motivated parametric models with interpretable inner structure combine prior knowledge with identification measurements. These bright-grey box models are the basis of several techniques related to control design (Schütte, 2003), observers, feed-forward and model-based fault diagnosis (Witczak et al., 2002).


The advantages of defining control parameters on the basis of physically motivated models as opposed to black-box models or completely model-free designs include:


1. simplicity, transparency,
2. online adaptability to changing parameters and model reference adaptive control (Khan et al., 2013; Riva et al., 2016),


3. optimality, e.g. pole placement, settling time,
4. predictability of robustness to changing system parameters,
5. low number of hyperparameters in the design, as opposed to modern H_∞ control (Toscano and Lyonnet, 2009).

In the industrial field of servo system control several model-based methods are widely known, but nevertheless model-less methods such as Ziegler-Nichols are still used to set the control parameters in most cases. A reason is that the selection of an appropriate model among a set of known candidates is a major difficulty and performance of model-based controllers hinges critically on the suitability of their models. For example, it may not be known a priori if elasticities in the structure should be considered or if they can be neglected. An attempt to perform a model selection including multiple-mass systems, backlash and friction is delineated in (Schütte et al., 1997), but it is not fully automatic. Models for control design tend to be rather simple, including only a few parameters. It is therefore important that the most dominant characteristics are identified as such which would require considerable effort and expert knowledge in practice if this task was performed manually. Especially when specialized systems such as stacker cranes, position-

^a <https://orcid.org/0000-0003-1195-7329>

^b <https://orcid.org/0000-0002-0512-1253>

^c <https://orcid.org/0000-0001-9161-0709>

^d <https://orcid.org/0000-0001-5605-9704>

This work was carried out as part of the research project "Automated Control Design based on (partly) automatically generated, Control-optimal Models" (FVA 665 IV), sponsored by the German Forschungsvereinigung Antriebstechnik e.V. (FVA)

ing systems and individual machine tools are commissioned in small quantities, model development comes at a comparatively high cost.

Methods for automatic model selection have been described (Aguilar et al., 2001; Tantau et al., 2020; Brun et al., 2001), which are mostly based on prediction accuracy as a sole criterion for goodness of the model, possibly in combination with parsimony requirements. Commonly, several models are identified and the one with the best fit on a separate validation dataset is nominated as the optimal model. Instead of separate validation data *information criteria* can be used (Chatfield, 1995). For servo systems with high quality actuators and sensors it can be expected that these stochastic criteria result in overly complex models, unlike the simple models known from control design. This suggests that accuracy is not a suitable model selection criterion in view of control design.

A control-relevant criterion for model selection is required. In the field of parameter identification control-relevant cost functions have been defined (identification for control) (Van Den Hof and Schrama, 1994; Hjalmarsson et al., 1996; Van den Hof, 1997; Gevers, 2004; Jansson, 2004; Codrons, 2005; Saha et al., 2021). Mostly, the overall aim is seen as to design a model-based controller with high performance on the real system and accordingly the optimal model is defined as the one with lowest performance degradation from model to real system or good worst-case performance (among other requirements). The cost function considers a given controller transfer function (Oomen et al., 2013) or if the controller transfer function is not known yet at the stage of identification, not even approximately, the v-gap metric is used for identification which allows to replace this knowledge by worst-case statements (Date and Vinnicombe, 2004; Geng et al., 2015; Yang et al., 2018).

One way to extend identification for control to model selection would be to use these control-relevant cost functions also for selection of the best model. This has been done in a few cases, see for example (van Herpen et al., 2010; van Herpen et al., 2011; Tacx et al., 2021; Tantau et al., 2022). This would favour again the most accurate models, where accuracy is measured in a special, control-relevant way. A slightly different approach is to also evaluate the nominal performance that can be achieved with each model, not only the performance degradation. This has already been considered in these references. In this sense the best model is the one with the potential to give a model-based controller the best performance on the real system. With this reasoning, the best model is not necessarily the most accurate one.

In this paper the idea of selecting the model that gives a model-based controller the highest performance is adopted, but the solution approach is very different, adopted to physically motivated models and common, industrial control design rules rather than \mathcal{H}_∞ -control. We propose to perform parameter identification for a couple of parametric models in a first experiment. Then, several commonly known controllers are parametrized for each model. Finally, the different resulting controller settings are validated on a non-parametric model in order to predict their stability and performance on the real system without actually carrying out hardware experiments, see below. The controller with the best performance defines the optimal model as the one that it is based on. Assuming that for each model the most promising controllers are tested, this procedure should output the model with potential to give a model-based controller the highest performance. What should facilitate applying this approach in industry, is that it is close to well known and established control design methods. The model selection strategy is similar to a manual model selection but more systematic and it requires less hardware experiments.

2 SET OF MODEL-BASED CONTROLLERS

In this section several commonly used model-based PI-controllers for speed control of electric motors with coupled mechanics are introduced briefly. They will be considered in the model selection of Sec. 4. Further details and derivations can be found in the cited references. Nonlinear characteristics are left out because the proposed method for model selection, see Sec. 3, can only handle transfer function models. The underlying transfer function models are identified in a first experiment as candidate models.

2.1 Symmetric optimum for systems with delay time

If elasticities in the mechanics can be neglected and the overall inertia of motor and load J_{sum} is the only parameter that describes the mechanics, a valid plant model is given by:

$$G(s) = \frac{1}{sJ_{\text{sum}}(1 + T_1s)}. \quad (1)$$

T_1 accounts for the limited sampling frequency in the current controller and the velocity measurement filter. In this case the PI-speed controller can be tuned according to the symmetric optimum in a way that the

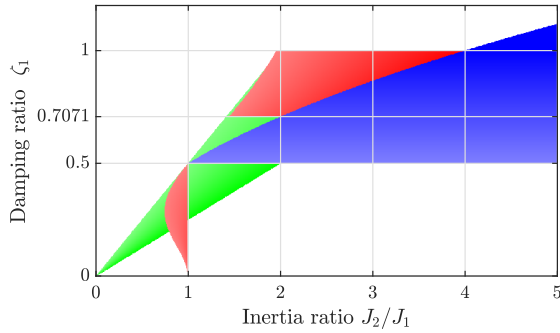


Figure 1: Chosen pole placement principles for 2-mass-systems. Blue: identical damping, red: identical real part, green: identical radius. When more than one principle is possible, identical damping is preferred over identical real part over identical radius.

zero-crossing frequency coincides with the maximum phase (Tripathi et al., 2015):

$$K_P = \frac{J_{\text{sum}}}{aT_1}, \quad T_1 = a^2 T_1. \quad (2)$$

a is a free parameter with the relation to the Lehr' damping ratio D of the closed-loop poles $a = 2D + 1$. $a = 2$ corresponds to optimal performance but $a = 3$ is more robust (Schröder, 2015). In the following experiments $a = 3$ is chosen.

Alternatively, the symmetric optimum can be designed for the first mass only of an elastically coupled system as a simple way to account for elasticity and transition elements with unknown properties such as belt drives and gear boxes. More advanced methods for multiple mass system control design are given next.

2.2 Pole placement for 2-mass-systems

Zhang (Zhang and Furusho, 2000) argues that for the two pole pairs of a controlled 2-mass-system there are three reasonable pole placement objectives: identical damping, identical real part and identical radius. Depending on the ratio of load inertia divided by motor inertia $R = J_2/J_1$ and the damping specified for the first pole pair ζ_1 these objectives may be achievable or not, see Fig. 1. In the figure a certain objective is considered achievable only if the damping ratio resulting for the second pole pair is 0.5 or more. For details see (Zhang and Furusho, 2000).

2.3 Optimal damping design for 2- or 3-mass-systems

Another popular controller design method, that has been used with 2-mass-systems, is the optimal damping design (Wertz and Schutte, 2000). It is based on

specifying *double ratios*. To obtain these the denominator polynomial of the closed control loop is written in the form

$$P(s) = a_n s^n + \dots + a_1 s + a_0. \quad (3)$$

Adjacent coefficients have the ratios $V_i = a_i/(a_{i-1}), i = 1 \dots n$. The double ratios are defined as $V_i/V_{i-1} = a_i a_{i-2}/a_{i-1}^2, i = 2 \dots n$, while the reciprocal values are sometimes called stability indices (Manabe, 1998). In (Manabe, 1998) it is recommended to aim for $D_{n-1} = \dots = D_2 = 0.5$ and $D_1 = 0.4$, as this gives the controlled system the properties of low overshooting, short settling time and a pole arrangement combining identical damping and identical real part. The control parameters can be chosen in fulfilment of these equations. If required, another defining equation can be generated by also specifying the system time $V_n = a_n/a_{n-1}$ (Schröder, 2015).

In the case of 2-mass-system speed control with PI-controller the denominator polynomial has five coefficients and three double ratios. Only the first two double ratios are specified to determine the two control parameters, because they are known to be more important than the last double ratios (Schütte, 2003). Out of the solutions one with positive real values is chosen which may not always exist.

For 3-mass-systems five double ratios exist and only two control parameters. Only the first two damping ratios are defined directly while the last three can assume arbitrary values.

3 MODEL SELECTION PROCEDURE

Having defined the candidate models and controllers in the preceding section this section explains the model selection procedure, starting with an overview followed by a more detailed description of certain points.

3.1 Description of the model selection method

The procedure can be outlined as follows:

1. Parameter identification for a set of physically motivated candidate models based on a measured frequency response function (FRF) of the system
2. Model-based control design / parametrization, as described in Sec. 2. For each model all potential controllers are parametrized.

3. Verification of all controllers via nonparametric models, as described in this section. The model corresponding to the best controller will be the best model.
4. Hardware tests of the resulting controller settings.

The parameter identification minimizes the sum of squared errors between model and plant FRF over all measured frequencies in the simplest case. The plant FRF, which is needed for this step, should be measured in a way that artefacts from the closed control loop are kept low, for example by inserting the excitation at r_1 in Fig. 2, while the controller is disabled. In the second step, if a certain controller cannot be parameterized for the given model parameters, e.g. because the control parameters would be complex, it is left out.

In the third step the various controllers are tested on a nonparametric model in order to predict their stability and performance on the real system without actually carrying out hardware experiments. It is assumed that for each model the most promising controllers are considered. Then, the best controller defines its model as the one that can give a model-based controller the highest performance.

Performance should not be measured in combination with the model that a certain controller is optimized for, because this would be a trivial test; the performance would be ideal mostly. Instead, conditions should be close to performing verification experiments on the real hardware. This leads to the application of complex, nonparametric models. Examples of nonparametric models are the impulse or step response or the frequency response function (FRF).

Stability is checked by evaluating the Nyquist criterion for the open loop consisting of plant FRF and controller transfer function.

Furthermore it would be desirable to know the step response so as to evaluate settling time, overshooting and integral criteria as performance measures. Time-domain signals are more intuitive for many operators. The step response can be calculated from the system's FRF, as explained in the next section, so that a nonparametric model is available for this kind of validation, too. Alternatively, time-domain signals could be obtained from the convolution of the system's impulse response (Risuleo, 2016).

Because of the linear nature of the transfer function nonlinear plant characteristics, e.g. friction, backlash, and saturation cannot be considered explicitly and it is expectable that the methods fail if they are dominant. Extensions to nonlinear models such as long short-term memory networks would be conceivable but the experimental effort for training seems inappropriate for simple PI control design.

3.2 Step response from frequency-domain measurements

As an evaluation of the model-based controllers with a nonparametric model step responses are calculated numerically. Using the measured FRF of the system together with the calculated transfer function (tf) of the controller this is a question of converting frequency-domain responses into a time-domain signals.

This could be done via inverse Laplace transform by calculating the *Bromwich inversion integral* (Grassmann, 2013):

$$f(t) = -\frac{1}{2\pi i} \int_{c-i\infty}^{c+i\infty} F(s)e^{st} ds, \quad (4)$$

in which c is a constant larger than the maximum real part of the poles of the Laplace transform $F(s)$. Methods for the numerical approximation of the integral can be found for example in (Hosono, 1981; Abate and Whitt, 2006; Gómez et al., 2007).

However, from the FRF the transfer function is only known for $c = 0$. Setting $c = 0$ the Fourier transform results (Grassmann, 2013):

$$f(t) = \frac{1}{2\pi} \int_{-\infty}^{\infty} F(i\omega)e^{i\omega t} d\omega. \quad (5)$$

Practically, it must be approximated via sum or trapezoidal integration method and only a finite maximal frequency can be considered. Further simplifications can be made if the time signal at negative times is not of interest, which is usually the case for causal systems (Tan et al., 2017).

The restriction to $c = 0$ forbids to calculate the time signal of transfer functions with nonnegative poles, for example undamped resonating systems or the s in the denominator introduced by the step excitation. Put differently, the signal in time must decay. It is therefore usually easiest to reconstruct the impulse response at first and to integrate it afterwards.

Another approach is to replace the step excitation by a periodic, mean-free square wave, e.g. periodic steps from -1 to 1 and from 1 to -1 and to assume that the system has been exposed to this excitation for a long time already. Now the system response $h(t)$ is periodic and can be calculated by means of Fourier series expansion, see derivation in (Tan et al., 2017):

$$h(t) = \frac{4}{\pi} \sum_{k=1(2)}^{\infty} \frac{1}{k} \operatorname{Re}\{F(ik\omega_s)\} \sin(k\omega_s t) \dots \\ + \frac{1}{k} \operatorname{Im}\{F(ik\omega_s)\} \cos(k\omega_s t). \quad (6)$$

$F(ik\omega_s)$ refers to the system for which the step responses are of interest. In the context of controller

validation $F(i\omega_s)$ is a spectral line of the closed feedback loop of plant and controller. The 2 in brackets means that every second frequency component is skipped. Note that the frequency component 0 is not evaluated, which in contrast to some other methods also allows to calculate the system response of systems with one pole in the origin, but the calculated system response is not quite correct in this case because initial conditions are neglected. These could lead to an arbitrary offset on the output which is not considered, instead $h(t)$ is always centred around 0. Apart from that the system should be stable.

Out of the step responses from -1 to 1 the step responses from 0 to 1 or between two other constants can be calculated by scaling the obtained results, as long as the (controlled) system has a limited and known static gain: The output offset will be the input offset times the static gain and the output amplitude will be the input amplitude times the static gain. This is related to the linearity of the considered systems, so an offset in the input will lead to a constant offset of known height in the output after settling motions have decayed. For an integrator the condition of a static gain is violated as the static gain is infinite.

This method can be implemented efficiently with the Matlab function *iff* leading to short calculation times.

Because in first experiments the integration of the impulse response showed to be inaccurate, in the following only the Fourier series method with square wave excitation is used, the accuracy of which will be demonstrated in Sec. 4. It is known that the conversion from frequency-domain measurements to time-domain signals is generally unstable and especially high-frequency oscillations can be introduced by minor errors in the measured transfer function (Doetsch, 1985). So the accuracy of the step response reconstruction will be pivotal in the remainder of the paper.

3.3 Calculation of the closed-loop system response in frequency-domain

The Fourier transform of the closed-loop control system, which is needed in (6), could be calculated from the plant FRF $P(i\omega)$ identified in open loop and the known controller TF $C_{\text{dest}}(s)$ (SISO case):

$$G_{\text{cl,dest}}(i\omega) = \frac{P(i\omega)C_{\text{dest}}(i\omega)}{1 + P(i\omega)C_{\text{dest}}(i\omega)}. \quad (7)$$

For the setup in Fig. 2 this means that r_1 is used to inject the excitation while $C(i\omega)$ is set to zero.

However, calculating the closed loop in this way would be inaccurate because the exact behaviour of

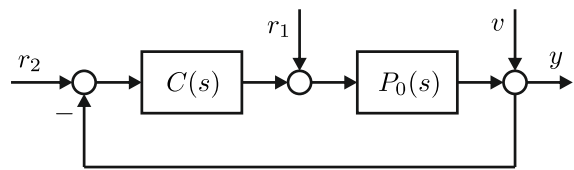


Figure 2: Control loop after (Van Den Hof and Schrama, 1994) with controller $C(i\omega)$, plant $P_0(i\omega)$, output y , measurement noise v and two possible excitations r_1 and r_2

the industrial drive C_{dest} is not known in detail (filters, resampling, time delay, etc.).

Instead, the closed loop is measured directly with excitation at r_2 for a given, working controller $C_{\text{origin}}(i\omega)$, which is ideally close to the controller to be designed, for example the default setting provided by the manufacturer. Calling this measured FRF $G_{\text{cl,origin}}(i\omega)$ the system's FRF is extracted via:

$$P(i\omega) = \frac{G_{\text{cl,origin}}(i\omega)}{C_{\text{origin}}(i\omega)(1 - G_{\text{cl,origin}}(i\omega))}. \quad (8)$$

Then the closed loop FRF is calculated for the to be designed controller via (7), using $P(i\omega)$ from (8). In this way the closed-loop FRF is still relatively accurate, even if the true controller transfer functions are not known exactly, at least when C_{origin} and C_{dest} are close. If they are even identical, insufficient knowledge about filters, resampling, time delay, etc will not lead to any errors. $P(i\omega)$ contains some of these distortions and is therefore not useful if one is interested in the FRF of the system alone.

This approach is in agreement with the claim of 'identification for control', which dictate to measure a system or to identify a model in a way that is close to the intended use of the model, resp. measurement. For example, if a model is needed for closed-loop predictions it should also be measured in closed loop (Gevers and Ljung, 1986; Van Den Hof and Schrama, 1994; Hjalmarsson et al., 1996; Van den Hof, 1997; Vinnicombe, 2001).

If at low frequencies $G_{\text{cl,origin}}(i\omega)$ is close to one or exactly one, then (8) cannot be calculated directly. In this case it is sufficient to note that $P(i\omega)$ is a very high number.

4 EXPERIMENTAL RESULTS

This section is intended to demonstrate the model selection procedure and the calculation of step responses from controller transfer function and non-parametric system model.



(a) Positioning stage with load on leaf springs



(b) Stacker crane

Figure 3: Experimental testbeds

4.1 Testbeds

Validation experiments are carried out on the two testbeds shown in Fig. 3. In the positioning stage a synchronous motor is connected to a toothed belt in direct drive moving a gantry with adjustable load. In addition, an extra load is mounted on leaf springs.

The stacker crane has a mast height of 5.6m and the x -axis is 5m long. All three axes are driven by synchronous motors with gearboxes and toothed belts. Experiments are carried out on the x -axis because due to mast oscillations and the elastic belt this

is the most challenging control design task. The y -axis is positioned constantly at 2000mm, 0 being the bottom end.

In both setups the motors are equipped with resolvers on the motor axis for position and velocity measurement. All motors, sensors and drives are of-the-shelf products from the company Lenze, which brings about a cascaded control structure (current, velocity, position). Position control is disabled, while the speed controller's TF is given by $C(s) = K_P(1 + 1/(T_I s))$. Its output is a torque, which is calculated into a current with the motor constant. Additional notch filters could be tuned for the commanded current but this possibility is not utilized here. The current controller is parametrized as recommended by the manufacturer.

4.2 Reconstruction of the step response from frequency-domain measurements

Before the results of the model selection are shown, the reconstruction of step responses for different controller settings is verified along measurements on the positioning stage testbed. The results for the stacker crane look similar, but they are not shown for the sake of brevity.

Following Sec. 3.3 and (8) the closed-loop FRF from desired velocity r_2 to actual velocity has been measured for $K_P = 0.0186 \text{ Nm}$, $T_I \rightarrow \infty$ one time with stepped sine, stepping from 0.5Hz to 500Hz. On this basis step responses have been reconstructed as described in Sec. 3.2 and Sec. 3.3 for different controller settings with the square wave method and alternating steps between -1 and 1 . The base frequency is 0.5Hz, so steps in either direction occur at 1Hz. Fig. 4, 5, and 6 show the resulting calculated step responses along with actually measured step responses for the respective controller settings. In order to qualitatively demonstrate the effect of nonlinearities and disturbances, two different step heights are shown each. For better comparison the calculated step responses are scaled to the same speed range as the measurements. Scaling is possible here because the static gain is known to be 1.

It can be seen that the calculated step responses resemble the measurements (overshooting, settling time, frequency of vibration) quite well. A noteworthy difference is the remaining oscillation in the measurement. This oscillation is synchronous with the motor angle (four peaks per revolution) and is therefore not part of the settling motion but rather a cause of a slight commutation misalignment of the current measurement. It shows the disturbance rejection /

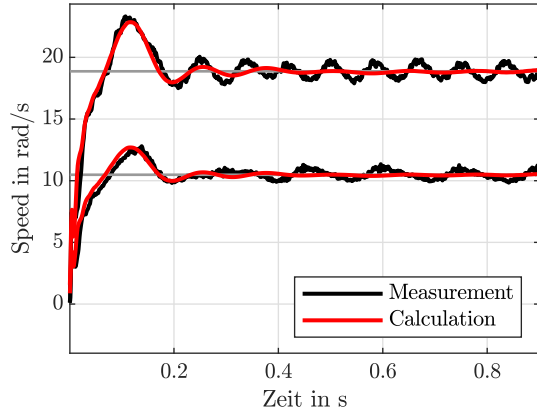


Figure 4: Measured and calculated step responses for two different step heights, $K_P = 0.0186 \text{ Nm/rpm}$, $T_I \rightarrow \infty$

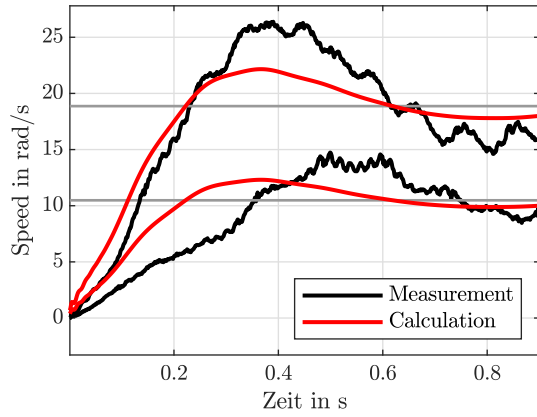


Figure 5: Measured and calculated step responses, $K_P = 0.00186 \text{ Nm/rpm}$, $T_I \rightarrow \infty$

amplification property, not the settling motion. Differences between the measurements for different step heights caused by nonlinearity can clearly be seen, especially for $t > 1 \text{ s}$ in Fig. 6. Deviations of this size should therefore also be expected between calculation and measurement. In Fig. 5 the overshooting is not captured precisely. This shows the lack of accuracy if C_{origin} and C_{dest} differ significantly in their controller settings (here factor 10).

4.3 Model selection for the positioning stage testbed

The identification of multiple mass models is carried out by inserting an excitation at r_1 , see Fig. 2, while position control is disabled and the speed control is kept at a low bandwidth (proportional gain set to a factor 100 below the usual value). Because of the low

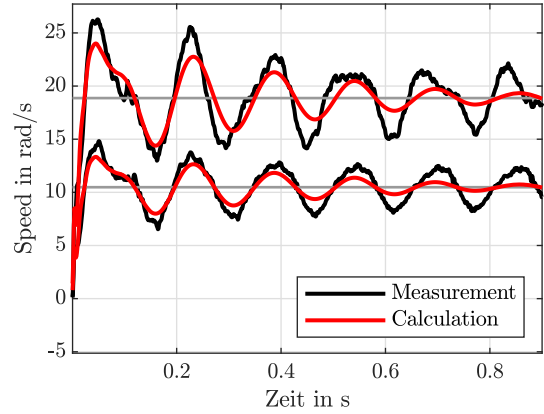


Figure 6: Measured and calculated step responses, $K_P = 0.0186 \text{ Nm/rpm}$, $T_I = 14 \text{ ms}$

bandwidth it can be ensured that every frequency line is excited sufficiently and the experiment is close to an open-loop experiment, leading to a smooth FRF measurement without significant closed-loop bias. The speed controller still prevents drifting of the integrating system.

A known PT1 element is included in all TF models with time constant T_I to account for the known sensor low-pass filter and current control, although a PT2 model would be more accurate. The known time constant is $T_I = 1.7 \text{ ms}$, 1.2 ms as sensor filter time constant and 0.5 ms for the current control.

Plant input and output (current and velocity) are evaluated with the Görtzel algorithm (Sysel and Rajmic, 2012) over several periods to average out measurement noise. The three different models shown in Fig. 7 have been identified by minimizing the mean squared distance in the complex plane over all recorded frequencies via particle swarm optimization. It can be seen that the 3-mass model fits best but at high frequencies a bias occurs in all models.

Based on these models the various controllers are calculated. The pole placement methods for 2-mass systems described in Sec. 2.2 could not be applied because the inertia ratio of the identified 2-MS is $\approx 0.5 < 1.0$.

In Fig. 8 the open-loop FRFs are shown as a first validation step. In addition, the default controller setting, provided by the manufacturer is shown for comparison. It is optimized for running the motor without load.

It can be seen that the symmetric optimum variants have insufficient gain margin. For this reason only the remaining three settings are further investigated by calculating the step response from the closed-loop FRF, measured with default controller settings, see Fig. 9. The colours correspond to Fig. 8.

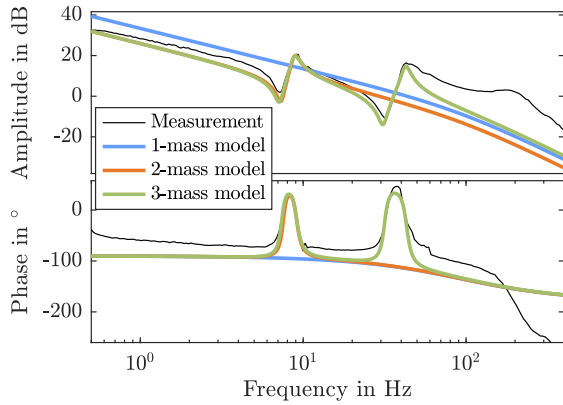


Figure 7: Plant FRF and identified models for the positioning stage

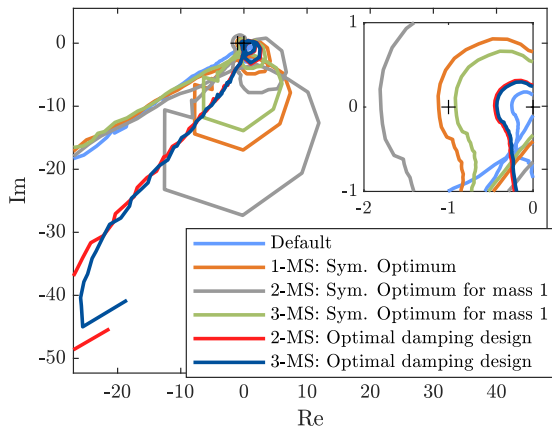


Figure 8: Nyquist plot for the considered set of model-based controllers, positioning stage testbed

Actually measured step responses are shown for comparison, normalized to steps from -1 to 1 . Because the red and the dark blue curve could hardly be distinguished, only the red curve is plotted.

Comparing the measured and calculated step responses it can be said that the frequency of oscillation and the decay ratio are in good agreement, whereas the overshoot is underestimated. Nevertheless, the evaluation of calculated step responses allows a first estimate. The exact shape of the step responses depends also on the step height due to nonlinearities, as shown in Sec. 4.2 and is therefore not captured precisely by the linear method.

Comparing the different control settings it can be seen that the optimal damping design achieves a clear improvement over the default setting and also the 1-mass model would not be appropriate. However, there is no clear answer to whether the 2-mass model or the 3-mass model should be favoured, because in this case both optimal damping designs lead to similar control parameters and therefore also similar performance.

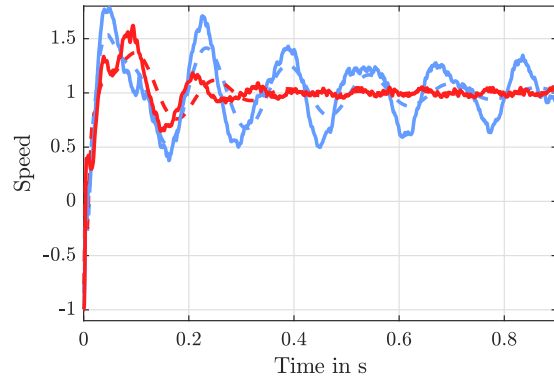


Figure 9: Calculated step responses for those settings that were approved in Fig. 8 (dashed) and corresponding measurements (continuous). The colours correspond to Fig. 8.

4.4 Model selection for the stacker crane testbed

Repeating the same workflow for the stacker crane testbed Fig. 10 shows the open loop locus for a number of control settings, see legend in Fig. 11. Some curves are not shown to keep the figure clean. The latter figure shows the calculated step responses. Error norms for the four admissible controller settings (sufficient gain margin in Fig. 10) are given in Tab. 1. The error norms for discrete-time signal y_k are defined as follows:

$$L_1 = \sum_k |y_k - 1|, \quad (9)$$

$$L_2 = \sqrt{\sum_k (y_k - 1)^2}, \quad (10)$$

$$\text{overshooting} = \max_k (y_k - 1). \quad (11)$$

Table 1: Performance criteria for the calculated step responses in m/s, stacker crane

	L_1	L_2	overs.
Default setting	114	5.7	0.344
3-MS: Sym. Optimum	76	3.88	0.199
2-MS: Optimal damping	111	6.73	0.299
3-MS: Optimal damping	142	8.22	0.238

Which controller and accordingly which model should be selected depends on the requirements of the application, but in this case it can be said that the symmetric optimum design based on the third mass of a 3-mass system is superior in all error norms. So, the control-optimal model for this testbed is clearly the 3-mass model.

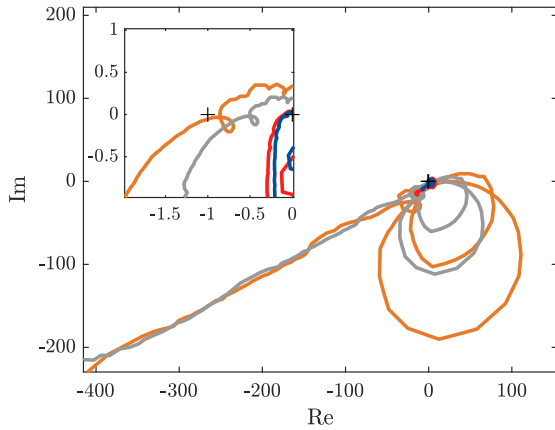


Figure 10: Nyquist plot for the considered set of model-based controllers, stacker crane

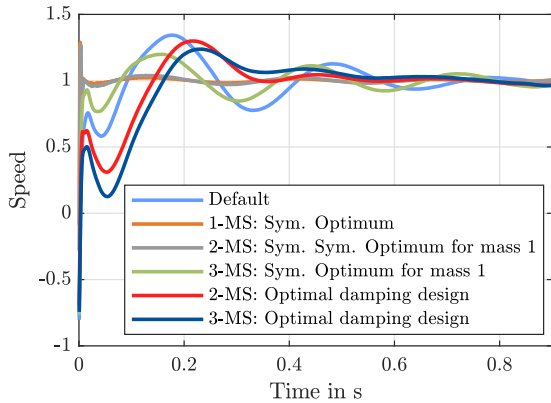


Figure 11: Calculated step responses for different model-based controllers, stacker crane

A comparison of measured and calculated step responses is shown in Fig. 12. The overall shape is in good agreement, except for additional scattering in the measurement which is assumed to be caused by backlash. So, although nonlinearity has a significant influence on the step response, the linear method does not fail. Merely the nonlinear artefacts are not predicted correctly.

5 DISCUSSION

This paper is intended to give a possible answer to the often asked question: Given a frequency-domain measurement of a system and several candidate models obtained from parameter identification, which model is the one to choose for control design? The proposed decision making comes at little expense as only one more experiment is required rather than several experiments (one for each controller-model combination). The reason why this second experiment is

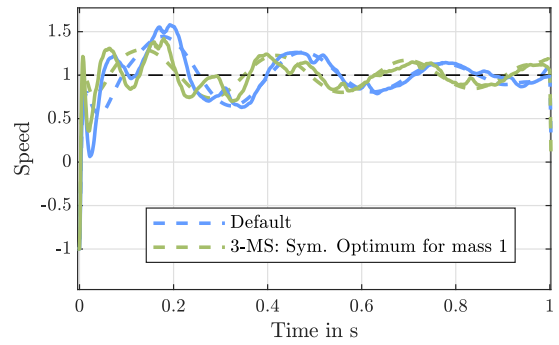


Figure 12: Calculated (continuous) vs. measured and scaled (dashed) step responses for two controller settings, stacker crane

necessary at all is twofold: Firstly, a higher accuracy of the verification with calculated step responses can be achieved by the special experiment in closed loop, as explained in Sec. 3.3, which is also expectable from the cited literature about identification for control. This theory says that a model should always be measured in a way that is close to its intended purpose. Secondly, model selection requires a separation into training and validation dataset. The second experiment constitutes the validation dataset and is therefore indispensable for a precise and unbiased performance scoring. A third dataset (test data) comprises of the measured step responses, which are not really part of the model selection method but serve as a validation of the method as a whole.

The results of the preceding section have demonstrated a fairly good accuracy of the step response calculation in spite of parasitic nonlinearities for two testbeds. These nonlinearities result from the fact that no ideal mass-spring-damper systems were tested but realistic, application-oriented setups with industrial hardware. This is especially true for the stacker crane.

Model selection was carried out successfully, although the simple PI control cannot fully utilize the relatively complex models. This is evident from the fact that all the step responses look relatively similar. In both examples the exact model is not as critical as one might expect from Fig. 7, where the models have a clearly different fit. The method cannot easily be extended to other controller transfer functions, possibly with higher order. For example, PID control cannot readily be incorporated because the suitability of the derivative feedback depends also on the sensors' signal quality, which cannot be taken into account easily. This is unfortunate because sometimes PID control can be an advantage over PI control (Zhang and Furusho, 2000). It could be investigated in future works if methods with more explicit

model-dependency like flatness-based control of 2/3-mass systems (Tkany et al., 2020) show a more significant difference between the models.

It should be highlighted that this model selection method is very close to existing approaches, where several physically motivated models are identified without any considerations about control-relevant excitation or control-relevant cost functions and then a commissioning engineer has to decide which model is most suitable. However, better results could possibly be obtained if the *parameter identification* of the candidate models was already carried out with special control-relevant cost functions, see for example (Codrons, 2005), not only the model selection. It can be seen in Fig. 7 that the parameter identification, as carried out in this paper, leads to bias errors in amplitude at high frequencies, where the phase is around -180° in Fig. 8. As a consequence of the inaccuracy some of the designed controllers are rendered inappropriate although they could possibly work well with a more accurate model. It is possible that a more specialized identification criterion could avoid this bias and instead introduce bias at less important frequencies. Considering control-relevant identification criteria could be future work.

Another problem is that the best controller for a certain model may not have been tested, because only a limited number of controllers is considered. Also, the parametrization of hyperparameters is sometimes arbitrary, for example the damping ratio. The possibility exists that for a different damping ratio a better performance could have been obtained. On the other hand, a completely manual model selection procedure would probably be suboptimal in the same way and the given procedure is still more systematic.

6 CONCLUSION

In the paper at hand a procedure was proposed to leverage state-of-the-art model-based controllers to realize a control-oriented model selection of first principle models for electric drives with imperfect mechanics. The goal is to select the model that leads to optimal performance of a model-based controller, not the most accurate model. A clear focus was laid on model selection rather than parameter identification. The model selection is based on open-loop frequency response functions and step responses for verification of the different model-controller combinations.

In experiments on two industrial testbeds it was shown that the step responses calculated with the nonparametric model predict the general shape accurately, while deviations still exist due to nonlinearities

and disturbances in the real system that are arguably not related to the settling motion. A clear improvement of the controller's performance over the default settings was achieved for one of the two testbeds. Limitations are the inability to consider sensor noise explicitly and the not control-optimal bias error in the parameter identification. The experiments have shown that the best model is not always the most accurate model, as expected. But it was found that often there is no sharp optimum and several models are almost equally good.

ACKNOWLEDGEMENTS

This work was sponsored by the German Forschungsvereinigung Antriebstechnik e.V. (FVA).

REFERENCES

- Abate, J. and Whitt, W. (2006). A unified framework for numerically inverting laplace transforms. *INFORMS Journal on Computing*, 18(4):408–421.
- Aguilar, J., Cerrada, M., and Cordero, A. T. F. (2001). Genetic programming-based approach for system identification. *Advances in Fuzzy Systems and Evolutionary Computation, Artificial Intelligence*, pages 329–334.
- Brun, R., Reichert, P., and Künsch, H. R. (2001). Practical identifiability analysis of large environmental simulation models. *Water Resources Research*, 37(4):1015–1030.
- Chatfield, C. (1995). Model uncertainty, data mining and statistical inference. *Journal of the Royal Statistical Society: Series A*, 158(3):419–444.
- Codrons, B. (2005). *Process modelling for control: a unified framework using standard black-box techniques*. Springer Science & Business Media.
- Date, P. and Vinnicombe, G. (2004). Algorithms for worst case identification in H_∞ and in the v-gap metric. *Automatica*, 40(6):995–1002.
- Doetsch, G. (1985). *Anleitung zum praktischen Gebrauch der Laplace-Transformation und der Z-Transformation*. R. Oldenbourg Verlag München, fifth edition.
- Geng, L.-H., Cui, S.-G., Zhao, L., and Lin, H.-Q. (2015). A convex optimization algorithm for frequency-domain identification in the v-gap metric. *International Journal of Adaptive Control and Signal Processing*, 29:362–371.
- Gevers, M. (2004). Identification for control: Achievements and open problems. *IFAC Proceedings*, 37(9):401–412.
- Gevers, M. and Ljung, L. (1986). Optimal experiment designs with respect to the intended model application. *Automatica*, 22(5):543–554.

- Gómez, P., Arellano, P., and Mota, R. O. (2007). Frequency domain transient analysis applied to transmission system restoration studies. In *Proc. of the 7th International Conference of Power Systems Transients (IPST'07)*.
- Grassmann, W. K. (2013). *Computational probability*, volume 24. Springer Science & Business Media.
- Hjalmarsson, H., Gevers, M., and De Bruyne, F. (1996). For model-based control design, closed-loop identification gives better performance. *Automatica*, 32(12):1659–1673.
- Hosono, T. (1981). Numerical inversion of laplace transform and some applications to wave optics. *Radio Science*, 16(6):1015–1019.
- Jansson, H. (2004). *Experiment design with applications in identification for control*. PhD thesis, Royal Institute of Technology (KTH), Stockholm, Sweden.
- Khan, M. B., Munawar, K., and Nisar, H. (2013). Switched hybrid position control of elastic systems with backlash. In *2013 IEEE International Conference on Control System, Computing and Engineering*, pages 551–556. IEEE.
- Manabe, S. a. (1998). Coefficient diagram method. *IFAC Proceedings Volumes*, 31(21):211–222.
- Oomen, T., van Herpen, R., Quist, S., van de Wal, M., Bosgra, O., and Steinbuch, M. (2013). Connecting system identification and robust control for next-generation motion control of a wafer stage. *IEEE Transactions on Control Systems Technology*, 22(1):102–118.
- Risuleo, R. S. (2016). *System identification with input uncertainties: an EM kernel-based approach*. PhD thesis, KTH Royal Institute of Technology.
- Riva, M. H., Dagen, M., and Ortmaier, T. (2016). Adaptive unscented kalman filter for online state, parameter, and process covariance estimation. In *American Control Conference (ACC)*, pages 4513–4519. IEEE.
- Saha, P., Egerstedt, M., and Mukhopadhyay, S. (2021). Neural identification for control. *IEEE Robotics and Automation Letters*, 6(3):4648–4655.
- Schröder, D. (2015). *Elektrische Antriebe-Regelung von Antriebssystemen*. Springer Vieweg, Berlin, Germany, fourth edition.
- Schütte, F. (2003). *Automatisierte Reglerinbetriebnahme für elektrische Antriebe mit schwingungsfähiger Mechanik*. Shaker.
- Schütte, F., Beineke, S., Grotstollen, H., Fröhleke, N., Witkowski, U., Rückert, U., and Rüping, S. (1997). Structure-and parameter identification for a two-mass-system with backlash and friction using a self-organizing map. In *European Conference on Power Electronics and Applications*, volume 3, pages 3–358.
- Sysel, P. and Rajmic, P. (2012). Goertzel algorithm generalized to non-integer multiples of fundamental frequency. *Journal on Advances in Signal Processing (EURASIP)*, 2012(1):1–8.
- Tacx, P., de Rozario, R., and Oomen, T. (2021). Model order selection in robust-control-relevant system identification. In *19th IFAC Symposium on System Identification*, volume 54, pages 1–6. Elsevier.
- Tan, N., Atherton, D. P., and Yüce, A. (2017). Computing step and impulse responses of closed loop fractional order time delay control systems using frequency response data. *International Journal of Dynamics and Control*, 5(1):30–39.
- Tantau, M., Jonsky, T., Ziaukas, Z., and Jacob, H.-G. (2022). Control-relevant model selection for servo control systems. In *International Conference on Control, Decision and Information Technologies*, pages 1–8, Istanbul, Turkey. IEEE. accepted.
- Tantau, M., Popp, E., Perner, L., Wielitzka, M., and Ortmaier, T. (2020). Model selection ensuring practical identifiability for models of electric drives with coupled mechanics. In *21st International Federation of Automatic Control (IFAC) World Congress*, Berlin, Germany.
- Tkany, C., Grotjahn, M., and Kühn, J. (2020). Flatness-based feedforward control of a stacker crane with online trajectory generation. In *2020 4th International Conference on Automation, Control and Robots (ICACR)*, pages 79–87. IEEE.
- Toscano, R. and Lyonnet, P. (2009). Robust pid controller tuning based on the heuristic kalman algorithm. *Automatica*, 45(9):2099–2106.
- Tripathi, S. M., Tiwari, A. N., and Singh, D. (2015). Optimum design of proportional-integral controllers in grid-integrated pmsg-based wind energy conversion system. *International Transactions on Electrical Energy Systems*, 26(5):1006–1031.
- Van den Hof, P. (1997). Closed-loop issues in system identification. *IFAC Proceedings*, 30(11):1547–1560.
- Van Den Hof, P. M. J. and Schrama, R. J. P. (1994). Identification and control-closed loop issues. *IFAC Proceedings*, 27(8):311–323.
- van Herpen, R., Oomen, T., and Bosgra, O. (2011). A robust-control-relevant perspective on model order selection. In *Proceedings of the American Control Conference*, pages 1224–1229. IEEE.
- van Herpen, R., Oomen, T., van de Wal, M., and Bosgra, O. (2010). Experimental evaluation of robust-control-relevance: A confrontation with a next-generation wafer stage. In *Proceedings of the American Control Conference*, pages 3493–3499. IEEE.
- Vinnicombe, G. (2001). On closed-loop identification: error distributions in the v-gap metric. In *40th IEEE Conference on Decision and Control*, volume 4, pages 3099–3103. IEEE.
- Wertz, H. and Schutte, F. (2000). Self-tuning speed control for servo drives with imperfect mechanical load. In *IEEE Industry Applications Conference*, volume 3, pages 1497–1504. IEEE.
- Witczak, M., Obuchowicz, A., and Korbicz, J. (2002). Genetic programming based approaches to identification and fault diagnosis of non-linear dynamic systems. *International Journal of Control*, 75(13):1012–1031.
- Yang, Z., Geng, L., and Yang, Y. (2018). A computationally efficient eiv models identification method using the v-gap metric. In *37th Chinese Control Conference (CCC)*, pages 1729–1734. IEEE.

Zhang, G. and Furusho, J. (2000). Speed control of two-inertia system by pi/pid control. *IEEE Transactions on industrial electronics*, 47(3):603–609.